

*Characterizations of Sol gel Synthesized (1-x)BZT-xBCT
Ceramics*

THESIS SUBMITTED IN PARTIAL FULFILMENT OF THE REQUIREMENTS FOR
THE DEGREE OF

Master of Science in Physics
by
Amlan Swetapadma Senapati

**Under the supervision of
Dr. Pawan Kumar Sharma**



**DEPARTMENT OF PHYSICS
NATIONAL INSTITUTE OF TECHNOLOGY, ROURKELA
2009-2011**



CERTIFICATE

THIS IS TO CERTIFY THAT THE THESIS ENTITLED
“*CHARACTERIZATION OF SOL GEL SYNTHESIZED (1-X)BZT-XBCT*”
SUBMITTED BY MISS. AMLAN SWETAPADMA SENAPATI IN PARTIAL
FULFILMENT OF THE REQUIREMENTS FOR THE AWARD OF MASTER
OF SCIENCE DEGREE IN PHYSICS AT NATIONAL INSTITUTE OF
TECHNOLOGY, ROURKELA, IS AN AUTHENTIC WORK CARRIED OUT
BY HER UNDER MY SUPERVISION AND GUIDANCE.

TO THE BEST OF MY KNOWLEDGE, THE MATTER EMBODIED IN THE
THESIS HAS NOT BEEN SUBMITTED TO ANY OTHER ORGANIZATION.

Date:

Prof. Pawan Kumar Sharma
Dept. of Physics
National Institute of Technology
Rourkela – 769008

Acknowledgements

I am heartily obliged to my guide Dr. Pawan Kumar Sharma, for his continuous guidance and motivation during the entire course of my project. I truly appreciate and value his esteemed guidance and encouragement from the beginning to the end of this thesis. I am indebted to him for having helped me shape the problem and providing insights towards the solution.

I am thankful to all the members of Electro-ceramic Lab., Dept. of Physics for their support.

I want to thank Miss Jasashree Ray, Mr. V.Senthil, Mr Barun Kumar Barik and Miss Santripti Khandhai, Tanmaya Barapanda for their necessary help. I also like to thank all the teachers and all PhD, M Tech(R) scholar for their valuable suggestions.

In particular, I would like to thanks my parents, friends and batchmates for their moral support.

Contents

	<u>Page No</u>
<i>Abstract</i>	5
Chapter 1 Problem Identification and Motivation	6 - 12
1.1 Problem Identification	7 - 10
1.2 Motivation	10-11
1.3 Objective	12
Chapter 2 Experimental Procedure	13 - 20
2.1 Synthesis Route	14 - 15
2.2 Synthesis and characterization Techniques	15 - 19
2.3 Synthesis and characterization of (1-x)BZT-xBCT compositions by sol gel route	19 - 20
2.4 Flowchart	21
Chapter 3 Results and Discussions	22
3.1 XRD Analysis	23 - 25
3.2 Density and Porosity Analysis	25 - 26
3.3 SEM Analysis	26 – 28
3.4 Dielectric Properties Analysis	28 - 32
3.3 Hystersis Loop Analysis	32 -36
Chapter 4 Conclusion	37 - 38
References	39

Abstract

Barium zirconate titanate – Barium calcium titanate [(1-x)BZT-xBCT] (48BZT-52BCT, 50BZT-50BCT, 52BZT-48BCT) ceramic were prepared by sol-gel method. The sample was calcined at 1100°C. The X-Ray diffraction of calcined powder showed the formation of single perovskite phase with no impurity peaks. 48BZT-52BCT, 50BZT-50BCT and 52BZT-48BCT were sintered at two temperatures i.e., 1200°C and 1300°C. The SEM images of the sintered pellets showed that the grain size varied from 800nm to 2µm. The dielectric property was studied under the frequency range from 100 Hz to 1 MHz and also by varying the temperature from 30°C to 200°C. The PE Loop of the sample was obtained by PE Loop tracer which confirmed the ferroelectric effect in 48BZT-52BCT, 50BZT-50BCT, 52BZT-48BCT ceramics.

Chapter 1: Problem Identification and Objective

1.1 Problem Identification:

Dielectrics are sub class of insulators. We know there are 32 point groups out of which 21 point groups are non-centro symmetric and 11 are having centre of symmetry. We are interested in these 21 groups as they posses dipoles. Again out of 21, 20 point groups (except 432 point group) show piezoelectric behaviour. Of these 20 point groups, 10 point groups have unique polar axis i.e., when we apply an electric field then they will polarize in a particular direction. Hence they exhibit pyroelectric effect. If the magnitude and direction of polarisation can be reversed then it is called ferroelectric material [1, 2].

1.1.1 Piezoelectricity:

It is the ability of materials to develop an electric charge proportional to mechanical stress called direct piezoelectric effect. Piezoelectric material also shows converse effect, where electric potential is developed on application of mechanical stress. This is an electromechanical phenomenon [1].

$$P_i = d_{ij}\alpha_{jk} \text{ (Direct Piezoelectric Effect)}$$

$$\beta_{ij} = d_{ij}E_k \text{ (Converse Piezoelectric Effect)}$$

Where,

P_i = polarisation along i-axis

α_{jk} = applied stress

d_{ij} = piezoelectric coefficient

β_{ij} = strain

E_k = electric field along k-axis

Piezoelectric properties are dependent on orientational direction, so they must be described in terms of tensors. A convenient way to specify the directional properties is to use subscripts that define the direction and orientation. Piezoelectric coefficients are usually indicated with two subscripts denoting the direction of the properties. The first subscript refers to the direction of the electric field E (or the displacement D). The second subscript refers to the direction of the mechanical stress α (or the strain h). For example, in d_{ij} , 'i' represents electric field or displacement direction and 'j' represents the stress or strain direction w.r.t the electric field direction.

Piezoelectric materials are used in transducers which converts one form of energy to other. The best-known application is the electric lighter. These are also used as actuators and sensors [1].

1.1.2 Pyroelectricity:

It is mentioned earlier that 10 out of 21 non-centro symmetry classes of materials shows spontaneous polarisation. And these spontaneous polarisations depend on temperature. This is called pyroelectric effect [2].

$$\Delta P_s = \Pi \Delta T$$

Where,

ΔP_s = spontaneous polarisation

Π = Pyroelectric co-efficient

ΔT = change in temperature

An increase in temperature leads to decrease in spontaneous polarisation. Polarisation suddenly falls to zero on heating above a particular temperature. This is because with increase in temperature thermal agitation increases, leading to opposition of the dipoles to align in particular direction.

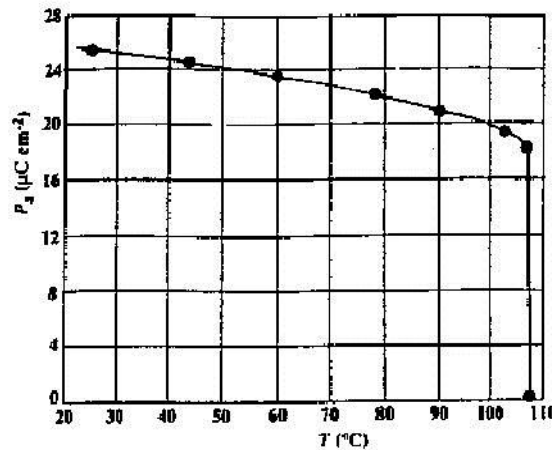


Fig. 1.1 The temperature dependence of spontaneous polarization P_s for $BaTiO_3$ ferroelectric crystal [3].

1.1.3 Ferroelectricity:

In pyroelectric material we have seen that the material is spontaneously polarised. But when this spontaneous polarisation magnitude and direction can be reversed by an external electric

field, then it is said to be ferroelectric. Therefore, materials that can be defined as ferroelectrics must have two characteristics: spontaneous polarisation and reversibility of polarisation under electric field. All ferroelectrics are pyroelectric and all pyroelectric are piezoelectric. Ferroelectric capacitors are indeed used to make ferroelectric RAM for computers, medical ultrasound machines.

These crystals contains called domains region inside which all electric dipoles are aligned in same directions. In a crystal there may be many domains separated by domain walls. The polarisation reversal can be observed by hysteresis loop.

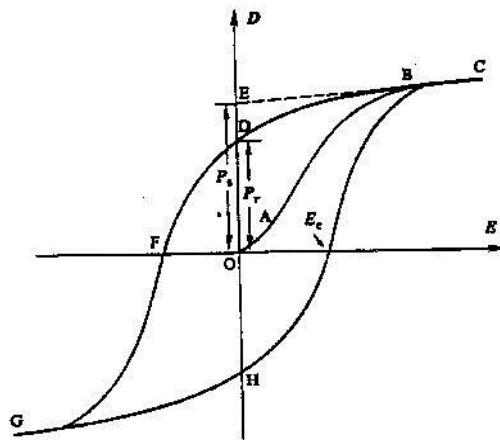


Fig. 1.2: A Polarization vs. Electric Field (P-E) hysteresis loop for a typical ferroelectric crystal [4].

As electric field strength increases, domains start to align in positive direction giving rise to rapid increase in polarisation (OB). At very high field polarisation reaches a saturation value (BC).The polarisation does not fall to zero when external field is removed (BO). At zero external field some of the domains remain aligned hence the crystal will show a remnant polarisation(P_r).The crystal cannot be completely depolarised until a field of magnitude(OF) is applied and this field is called coercive field(E_c). If the field is increased to more negative value direction of polarisation flips and hence a hysteresis loop is obtained [2].

It is mentioned earlier that beyond certain temperature, the material is no more ferroelectric. This particular temperature is called Curie point (T_c). So temperature $T > T_c$ crystal do not exhibit ferroelectricity. On decreasing the temperature below Curie point crystal undergoes phase transition from non-ferroelectric phase to ferroelectric phase. If there are more ferroelectric phases the temperature at which crystal changes from one ferroelectric phase to other is called transition temperature. Near the Curie point or transition temperature some

properties like dielectric, elastic, optical and thermal constants shows an anomalous behaviour, due to phase change [5, 6].

Ferroelectric ceramics are classified into ferroelectrics with bismuth layered-structure, tungsten bronze and perovskite structures.

Of these perovskite is more important because large numbers of ferroelectrics are under this category as its structure is simple and its properties can be tailored by substituting different element.

Piezoelectric materials generate a voltage when subjected to mechanical stress. This turns out to be a very useful property, endowing itself to applications from the common microphone and loudspeaker to scientific instruments such as atomic force microscopes, sensors, actuators. The most efficient piezoelectric materials are those that produce the most charge for a given force, like Lead Zirconate Titanate (PZT) containing lead, which is coming under increasingly tight regulation because of its high toxicity.

While lead-free piezoelectric do exist, but their performance is only a fraction of that of their lead-bearing counterparts. While, PZT has $d_{33} = 500\text{--}600$ pC/N, non-lead piezoelectric ceramics have inferior piezoelectricity i.e., $d_{33} < 150$ pC/N in most cases. Recently, their limit has been pushed to a higher level of $d_{33} = 300$ pC/N but is still halfway to the most-desired high-end PZT property [7, 8, 9].

Various studies on lead free material have been done, but their piezoelectric properties are far more inferior to the PZT. For example, KNN-LT ($\text{KNbO}_3\text{-LiTaO}_3$) and KNN-LN ($\text{KNbO}_3\text{-LiNbO}_3$) have piezoelectric coefficient $d_{33} = 150\text{--}300$ pC/N. Moreover the flaw with KNN-LT and KNN-LN is that it is costly to synthesize as it needs expensive elements La, Ta [10].

1.2 Material Selection:

Thus the essential requirements for good lead free piezoelectric ceramics are:

1. It should not contain lead.
2. It should have high Piezoelectric co-efficient.
3. It should have Morphotrophic Phase Boundary (MPB).

The MPB causes the instability in polarization phase so that the polarization direction can easily be rotated by electric field or external stress [11, 12].

The above requirements are very well satisfied by (1-x)BZT-xBCT ceramic. It is lead free and the piezoelectric constant (d_{33}) is around 600 pC/N. Along with this, the added advantage of (1-x)BZT-xBCT from other lead free system is the existence of C-R-T triple point [10].

It is noted that the existence of C-R-T triple point characterizes many highly piezoelectric Pb-based systems such as PZT and PMN-PT [10].

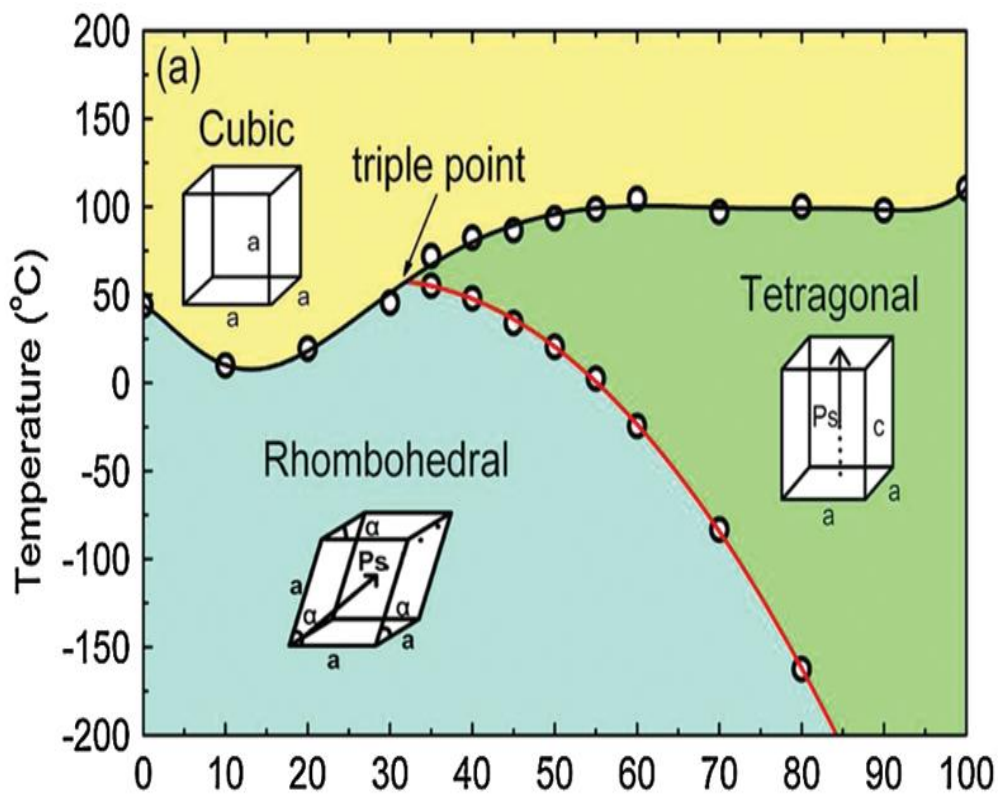


Fig. 1.3: Phase diagram of BZT-BCT [10].

Where,

C = Cubic Paraelectric

R = Rhombohedral Ferroelectric

T = Tetragonal Ferroelectric

1.3 Objectives:

The objectives and motives of the experiment carried out are listed below:

1. To synthesize 48BZT-52BCT, 50BZT-50BCT, 52BZT-48BCT ceramic near MPB by sol gel route.
2. To optimize the synthesis route.
3. To carry out various characterization on 48BZT-52BCT, 50BZT-50BCT, 52BZT-48BCT ceramic like X-Ray Diffraction, SEM, PE Loop measurement and Dielectric measurement.
4. To compare the properties of (1-x)BZT-xBCT ceramic prepared by solid state reaction method and sol gel route.
5. To suggest the best composition of (1-x)BZT-xBCT near MPB boundary.

The ways of achieving these objectives are discussed in further chapters.

Chapter 2: Experimental Procedure

2.1 Synthesis Routes:

There are various ways of synthesis of ceramic materials of those solid state reaction methods and sol gel method is of great importance and is widely used.

A solid state reaction, also called a dry media reaction or a solvent less reaction. It has got high reaction rate. These are mainly used for bicarbonates and oxides precursors. It has lower reaction temperature and it eliminate the chances of presence of intermediate impurity phases.

In this method, reactants should mix to a homogeneous system is a problem. It is more difficult to work with as it is hard to control exact stoichiometric in certain cases. Sometimes it is not possible to find compatible reagents for the reaction. In solid state reaction method, it is difficult to get fine particle size, so mixing forms an important step in this route. Therefore time and energy is invested in ball milling, the most popular way of mixing.

The sol-gel process, also known as chemical solution deposition, is a wet-chemical technique. It is mostly used for precursors like metal alkoxides and chlorides. In this chemical procedure, the 'sol' (or solution) gradually evolves towards the formation of a gel-like diphasic system containing both a liquid phase and solid phase whose morphologies range from discrete particles to continuous polymer networks [13].

This sol, which is a solution containing particles in suspension, is heated at low temperature to form a wet gel. This solution is densified through a thermal annealing. The sol-gel technique is based on hydrolysis of liquid precursors and formation of colloidal sols. Since the early steps of the sol-gel process occur in liquid phase, it is possible to add basically any substance (as solutions or suspensions) at this stage. Simple mixing provides uniform distribution of the dopant within the liquid host phase. After the gelation the guest molecules become physically entrapped within the now solid host matrix. Furthermore, the hydrolysis, doping and gelation occur usually at ambient temperatures. The doped matrices usually possess good optical characteristic like transparency and high refractive indices. Another advantage of the sol-gel method is its versatility and the possibility to obtain highly pure materials, the composition of which is perfectly controlled [14]. The grain size obtained in this way is also very small so the manual labour in grinding and reducing the grain size is lowered. As a result, the sintering and calcining temperature is lowered.

It has to be noted that bulk sol-gel samples suffer very often from internal cracks, leading to their destruction [14]. The choice of solvent is another issue that is needed to be taken care of in this route.

So, seeing both the advantages and disadvantages of solid state reaction method and sol gel method, in order, to get a purified low temperature sintered and calcined sample, we prefer sol gel method.

The chemical formula for $(1-x)\text{BZT}-x\text{BCT}$ is $(1-x)\text{Ba}(\text{Zr}_{0.2}\text{Ti}_{0.8})\text{O}_3-x(\text{Ba}_{0.7}\text{Ca}_{0.3})\text{TiO}_3$. We have taken three composition of $(1-x)\text{BZT}-x\text{BCT}$, as the region around 1:1 ratio of BZT and BCT ceramic is the region of MPB. So, the properties are at its best in this particular region. The three compositions of $(1-x)\text{BZT}-x\text{BCT}$ system in and around the region of MPB are:

1. $48\text{Ba}(\text{Zr}_{0.2}\text{Ti}_{0.8})\text{O}_3-52(\text{Ba}_{0.7}\text{Ca}_{0.3})\text{TiO}_3$ - (48BZT-52BCT)
2. $50\text{Ba}(\text{Zr}_{0.2}\text{Ti}_{0.8})\text{O}_3-50(\text{Ba}_{0.7}\text{Ca}_{0.3})\text{TiO}_3$ - (50BZT-50BCT)
3. $52\text{Ba}(\text{Zr}_{0.2}\text{Ti}_{0.8})\text{O}_3-48(\text{Ba}_{0.7}\text{Ca}_{0.3})\text{TiO}_3$ - (52BZT-48BCT)

2.2 Synthesis and characterization Techniques:

Synthesis of ceramic materials highly influences its properties. Intensive care and high purity should be maintained in the various steps of synthesis. The significance of each step followed in sol gel route is discussed below along with the various characterization techniques involved.

2.2.1 Synthesis Route:

The compositions 48BZT-52BCT, 50BZT-50BCT and 52BZT-48BCT are prepared by sol gel route.

2.2.1.1 Solution Preparation:

The raw materials are to be dissolved in suitable solvent in sol-gel method. The choice of solvent is very important. Solvent should be such that it completely dissolves in the solute and should also evaporate on heating, to serve this purpose organic solvents are the best. They should be non-reactive with the precursors, so that no new product should be formed due to the solvent. The dissolving of precursor in the solvent causes its particle size to be reduced; this can be understood from the transparency of the solution. The effect of this is the manual labour

in grinding is saved and the sintering and calcining temperature is lowered. The material formed will be of great purity. But, what matters is the choice of solvent.

2.2.1.2 Calcination:

Calcination is a thermal treatment process in order to bring about phase transition. The objective of calcination is usually:

1. To drive off water, present as absorbed moisture
2. To drive off carbon dioxide, sulphur dioxide, or other volatile constituent
3. To reduce volume or increase density.

This process takes place below the melting point of the material. This is the temperature at which Gibb's free energy is zero. Calcination temperature is important as it influences the density and so the electromechanical properties of final product. During this step, solid phase reaction takes place between the constituents giving ferroelectric phase .

2.2.1.3 Sintering:

Sintering is the processing technique used to densify the material by applying thermal energy. Through sintering we can control the grain size and density. In sintering grain bodies are heated to high temperature, but below the melting point, so that high rate of diffusion takes place. The driving force for sintering is the reduction in surface free energy of the system. So the reduction in energy causes the matter to transfer from grain boundaries to pores, and hence densifies the material.

2.2.2 Characterization Techniques:

The various characterization techniques followed after synthesis are discussed below.

2.2.2.1 X-Ray Diffraction (XRD):

This is a characterisation process. XRD is mainly used for the fingerprint characterisation of the material and determination of their structure. Crystals are regular arrays of atoms and X-rays are electromagnetic waves. When these X-rays strike atoms they scatter in different directions. In few directions these waves follow Bragg's law,

$$n\lambda = 2d \sin \theta,$$

Each material has its unique X-ray powder diffraction pattern which may be used as a fingerprint for its identification. Once the material is identified, X-ray crystallography is used

to determine its structure. From XRD, we can infer how the atoms are packed in the crystal, interatomic distance, angle, phase composition. So, to determine the structure and trace the fingerprint of the material, it is subjected to XRD [15].

2.2.2.2 Density Measurement:

Density measurement is based on Archimedes principle which states that an object is immersed in a fluid is buoyed up by a force equal to the weight of the fluid displaced by the object. Here the sample's weight is measured initially. The sample is then soaked in a solvent, after that again the weight is measured. So,

$$\text{Density} = [\text{Dry weight} / (\text{Soaked Weight} - \text{Suspended Weight})] * \text{specific gravity of solvent.}$$

From this data, we can also calculate porosity. Porosity is inversely proportional to density. Pores affect the strength of ceramic; they produce stress as a result crack is developed [16]. Presence of porosity also reduces the dielectric constant.

The working formula for the calculation of porosity is given below,

$$\text{Apparent Porosity} = [(\text{Soaked Weight} - \text{Dry Weight}) / (\text{Soaked Weight} - \text{Suspended Weight})] * 100 \%$$

2.2.2.3 Scanning Electron Microscope (SEM):

SEM is used for inspecting topographies of specimens at high magnifications. It is used in the analysis of cracks and fracture surfaces, bond failures and physical defects.

In a typical SEM, an electron beam is thermionically emitted from an electron gun fitted with a tungsten filament cathode. When the primary electron beam interacts with the sample, the electrons lose energy by repeated random scattering and absorption by the specimen. The energy exchange between the electron beam and the sample results in the reflection of high-energy electrons by elastic scattering, emission of secondary electrons by inelastic scattering and the emission of electromagnetic radiation, each of which can be detected by specialized detectors.

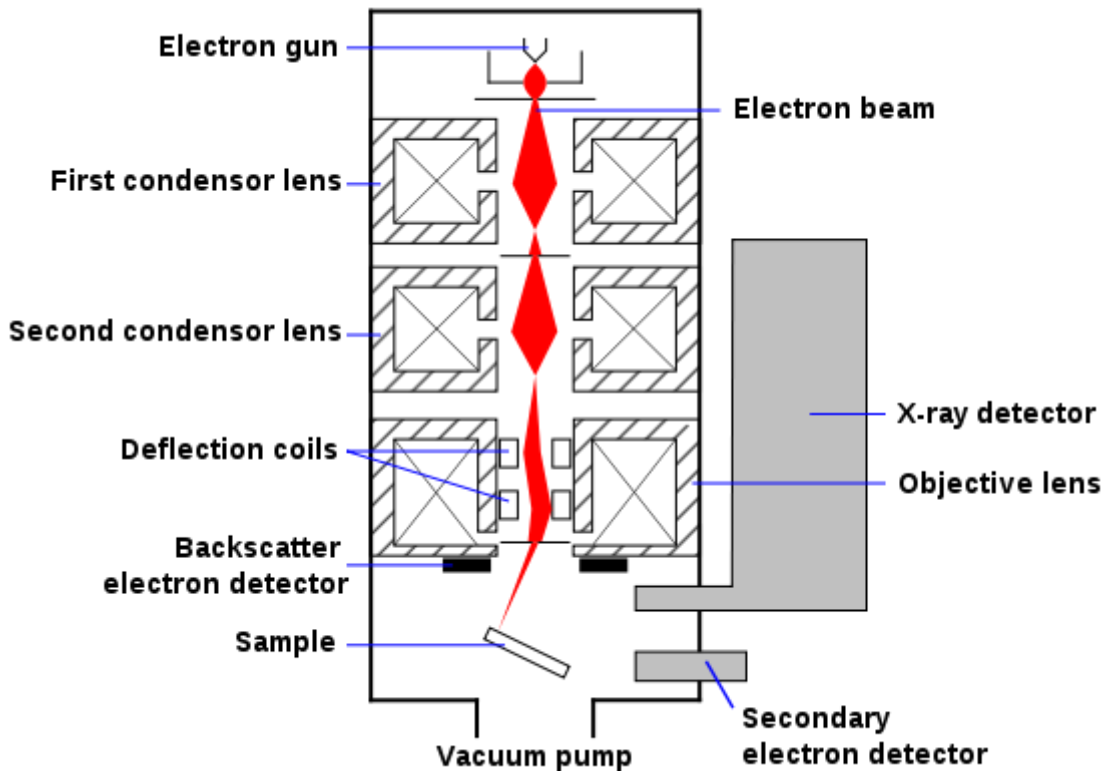


Fig. 2.2.2.3 Schematic SEM Diagram

Here we use the secondary electrons, which are converted into signals. SEM magnification can go to more than 10^6 magnitudes.

2.2.2.4 Dielectric Measurement:

LCR meters are generally used for measurement of the capacitance, dissipation factor and dielectric constant of Capacitors. LCR meter is based on the principle of automatic balancing bridge method.

2.2.2.5 PE Loop Tracer :

The ferroelectric material is characterised by its hysteresis loop. This loop is verified in the PE loop tracer. The instrument is based on modified Sawyer-Tower circuit. The principle of this instrument is that the function generator applies an alternating voltage across the capacitor stack, forcing charge onto the top plate of the ferroelectric capacitor. The same amount of charge will be forced to leave the opposite plate of the ferroelectric capacitor and collect on the top plate of the linear sense capacitor. According to the equation " $Q = CV$ ", the voltage across the linear sense capacitor will thus represent the number of electrons that move into or out of the ferroelectric capacitor as a result of the applied waveform. This measurement is usually

carried out at low frequency. Thus PE loop tracer checks whether the material is ferroelectric or not.

2.3 Synthesis and characterization of (1-x)BZT-xBCT compositions by sol gel route:

For BZT-BCT, the raw materials used are Barium acetate($\text{Ba}(\text{CH}_3\text{COO})_2$), Zirconyl nitrate hydrate($\text{ZrO}(\text{NO}_3)_2 \cdot x\text{H}_2\text{O}$), Calcium acetate ($\text{Ca}(\text{CH}_3\text{COO})_2$) with molecular weight 55.43gms, 249.25gms, 158.17gms respectively and for Titanium isopropoxide ($\text{C}_{12}\text{H}_{28}\text{O}_4\text{Ti}$) the density is 0.955 gm/cm^3 . So its molecular weight is 284.22 gms.

The amounts of raw materials required for 10 gms of all three systems are given below:

52BZT-48BCT:

$$\text{Ba}(\text{CH}_3\text{COO})_2 = 4.2077 \text{ gms}$$

$$\text{Ca}(\text{CH}_3\text{COO})_2 = 0.3926 \text{ gms}$$

$$\text{ZrO}(\text{NO}_3)_2 \cdot x\text{H}_2\text{O} = 0.4988 \text{ gms}$$

$$\text{C}_{12}\text{H}_{28}\text{O}_4\text{Ti} = 5.13168 \text{ ml}$$

50BZT-50BCT:

$$\text{Ba}(\text{CH}_3\text{COO})_2 = 4.1632 \text{ gms}$$

$$\text{Ca}(\text{CH}_3\text{COO})_2 = 0.4548 \text{ gms}$$

$$\text{ZrO}(\text{NO}_3)_2 \cdot x\text{H}_2\text{O} = 0.4770 \text{ gms}$$

$$\text{C}_{12}\text{H}_{28}\text{O}_4\text{Ti} = 4.9044 \text{ ml}$$

48BZT-52BCT:

$$\text{Ba}(\text{CH}_3\text{COO})_2 = 4.1369 \text{ gms}$$

$$\text{Ca}(\text{CH}_3\text{COO})_2 = 0.4734 \text{ gms}$$

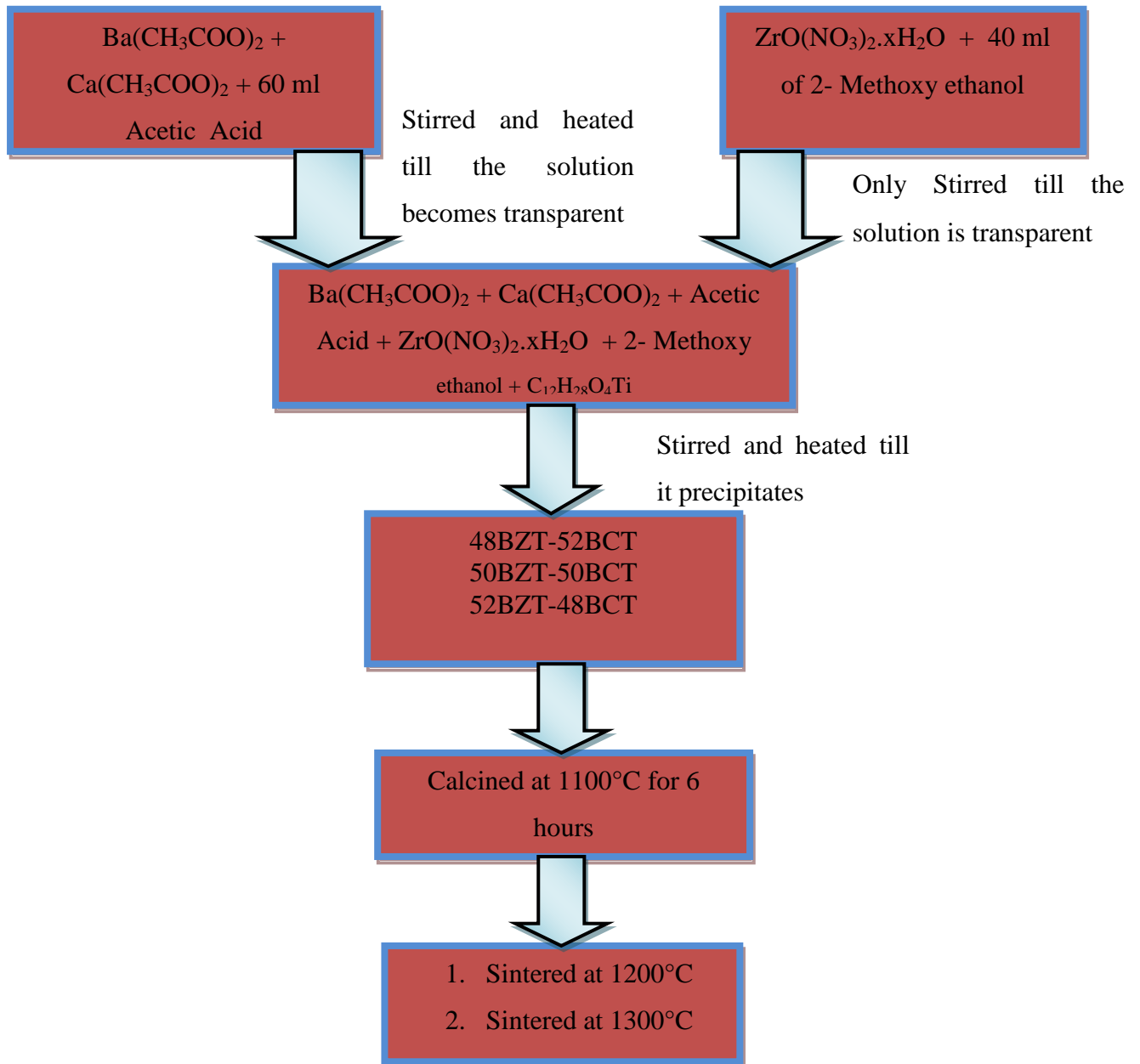
$$\text{ZrO}(\text{NO}_3)_2 \cdot x\text{H}_2\text{O} = 0.4591 \text{ gms}$$

$$\text{C}_{12}\text{H}_{28}\text{O}_4\text{Ti} = 5.1627 \text{ ml}$$

Barium acetate and Calcium acetate is soluble in Acetic acid. So the required amount of Barium acetate and Calcium acetate is dissolved in 60 ml of Acetic acid. It is placed on magnetic stirrer for half an hour, till the solution becomes transparent. $\text{ZrO}(\text{NO}_3)_2 \cdot x\text{H}_2\text{O}$ is soluble in 2- Methoxy ethanol. The solution should not be heated, but only stirred as it forms precipitation on heating. This solution of $\text{ZrO}(\text{NO}_3)_2 \cdot x\text{H}_2\text{O}$ and 2- Methoxy ethanol was added to the earlier solution of $\text{Ba}(\text{CH}_3\text{COO})_2$, $\text{Ca}(\text{CH}_3\text{COO})_2$ and acetic acid. $\text{C}_{12}\text{H}_{28}\text{O}_4\text{Ti}$ was pipetted to the above solution. This solution was continuously stirred and heated for about 4 hrs

so that precipitate was formed. The remnant lumps were removed by simple grinding for 10 minutes. All the three compositions i.e., 48BZT-52BCT, 50BZT-50BCT and 52BZT-48BCT were calcined in tubular furnace for 1100° C for 6 hours. The lumps formed during calcining process were grinded. The phase analysis is done using X-Ray Diffraction(Model: PW 1830 diffractometer, Phillips, Netherland) with filtered 0.154 nm Cu K α radiation in continuous mode from 20° - 70° with a scanning rate of 3°/min. Before shaping the powder into pellets, we have to mix binder. The binder used here is polyvinyl alcohol. The desired shape to the powder is given through powder compaction method. The pressure maintained is 60 tons for pellets preparation. Once the shaping of the material is done, binder is of no use. Therefore, to remove the binder we have to heat the pellets for 1 hour at 600°C. To densify the pellets, it is sintered at 1200°C and 1300°C for 4 hours. Density measurement is done by taking Kerosene as solvent whose specific gravity is 0.81. After density measurement, one important characterization is done which is useful in extracting information about the topography of the material i.e., SEM. Topographical features were studied using Scanning Electron Microscope (JSM 6480 LV JEOL, Japan). A thin layer of silver paste is applied on the surface of pellets. The dielectric measurement is done using HIOKI 3532 – 50 LCR Hi TESTER. Two measurements are done through LCR meter; one is the variation of dielectric constant (ϵ_r) with temperature. The temperature here is varied from room temperature to 200°C with 2° rise per minute. Second one, is the variation of ϵ_r and loss with frequency. The frequency is varied from 100 Hz to 1MHz. Necessary precaution to be taken is the silver paste continuity. To check the ferroelectric nature of the sample, it is introduced to Sower-Tower Circuit.

2.4 Flowchart:



Chapter 3: Results and Discussions

3.1 XRD Analysis:

The XRD plot of the calcined sample is given below.

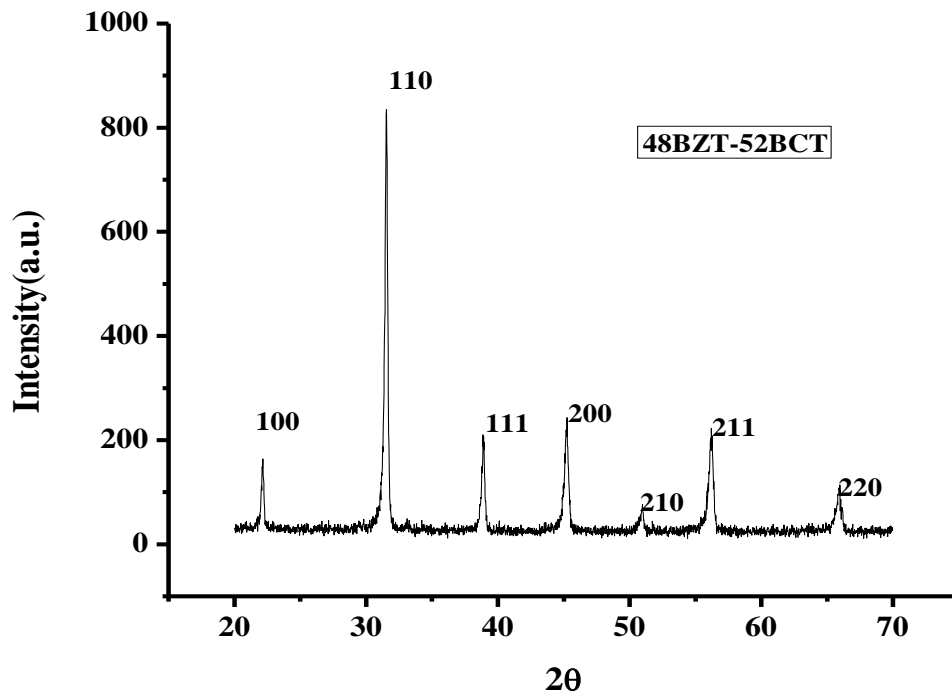


Fig.3.1.1 XRD Plot of calcined sample 48BZT-52BCT

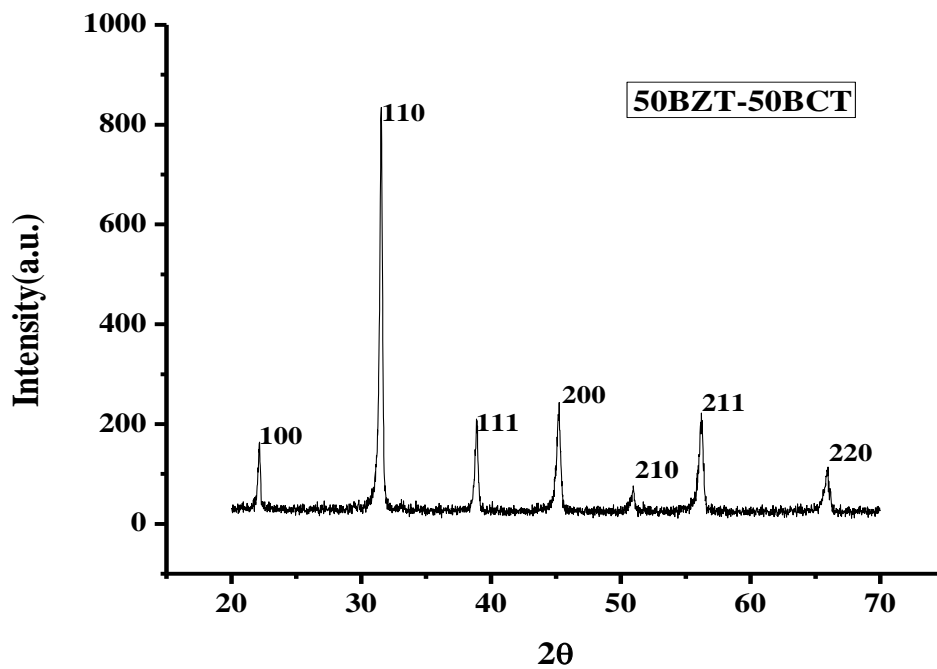


Fig.3.1.2 XRD Plot of calcined sample 50BZT-50BCT

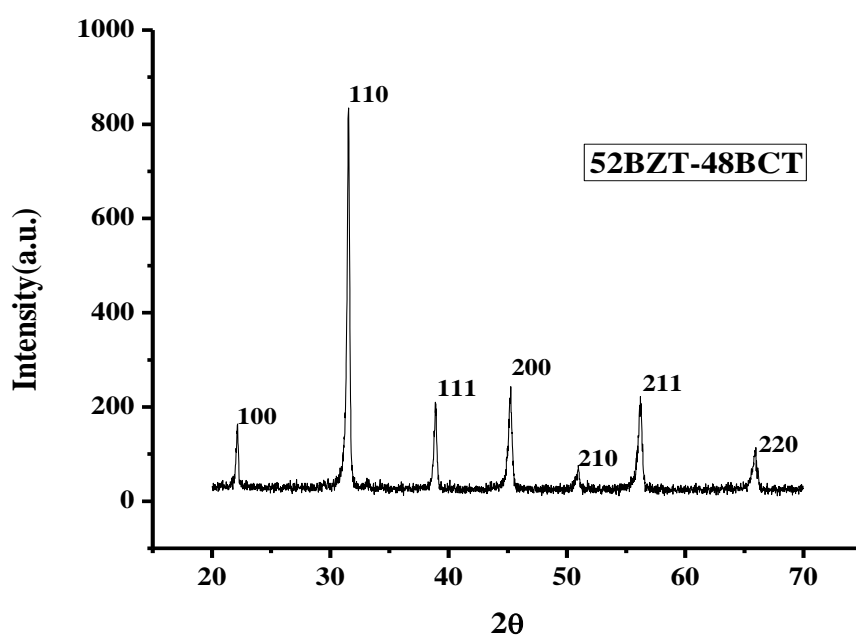


Fig. 3.1.3 XRD Plot of calcined sample 52BZT-48BCT

The Fig., 3.1.1, 3.1.2 and 3.1.3 represents the XRD plot of 48BZT-52BCT, 50BZT-50BCT and 52BZT-48BCT calcined sample at 1100°C. The prominent peaks in XRD plots are indexed to its respective hkl planes. From the above three plots, we infer that there is single perovskite phase formation without any impurities present.

The x-ray diffraction data so obtained were further subjected to refinement method. Here, substrate background was done. The value of $K\alpha_2$ was stripped and XRD plot was smoothened. Lastly, peak search was done through expert high score. The data obtained on refinement is tabled below.

Table -3.1.1

Sample Name	Crystal System	Space Groups	Lattice Parameters
48BZT-52BCT	Cubic	Pm3m	a=b=c=4.0159Å $\alpha=\beta=\gamma=90^\circ$
50BZT-50BCT	Cubic	Pm3m	a=b=c=4.0069Å $\alpha=\beta=\gamma=90^\circ$
52BZT-48BCT	Cubic	Pm3m	a=b=c=4.0060Å $\alpha=\beta=\gamma=90^\circ$

From the above table, we conclude that the three compositions of BZT-BCT system belongs to cubic crystal system with space group Pm3m.

3.2 Density and Porosity Analysis:

The density and porosity values of 48BZT-52BCT, 50BZT-50BZT and 52BZT-48BCT sintered at 1200°C and 1300°C are given below:

Temperature 1300°C:

Table-3.2.1

Sample	Dry Weight (gms)	Suspended Weight(gms)	Soaked Weight(gms)	Bulk Density	Apparent Porosity (%)
48BZT-52BCT	0.2836	0.2444	0.3186	3.0959	47.1699
50BZT-50BCT	0.2283	0.1969	0.2366	4.6580	20.9068
52BZT-48BCT	0.2620	0.2249	0.2720	4.5057	21.2314

Temperature 1200°C:

Table – 3.2.2

Sample	Dry Weight(gms)	Suspended Weight(gms)	Soaked Weight(gms)	Bulk Density	Apparent Porosity(%)
48BZT-52BCT	0.3024	0.2600	0.3428	2.9582	48.7922
50BZT-50BCT	0.2244	0.1929	0.2400	3.8591	33.1210
52BZT-48BCT	0.2354	0.2033	0.2488	4.1906	29.4505

Here we can infer that when density increases, porosity decreases. The main objective of sintering is to densify the pellets, which is verified by density measurement. From the above tables 3.2.1, 3.2.2, we conclude that the density of the samples sintered at 1300°C is better than that of 48BZT-52BCT, 50BZT-50BCT, 52BZT-48BCT compositions sintered at 1200°C.

3.3 SEM Analysis:

The SEM images of 48BZT- 52BCT, 50BZT-50BZT and 52BZT- 48BCT sintered at 1300°C are given below.

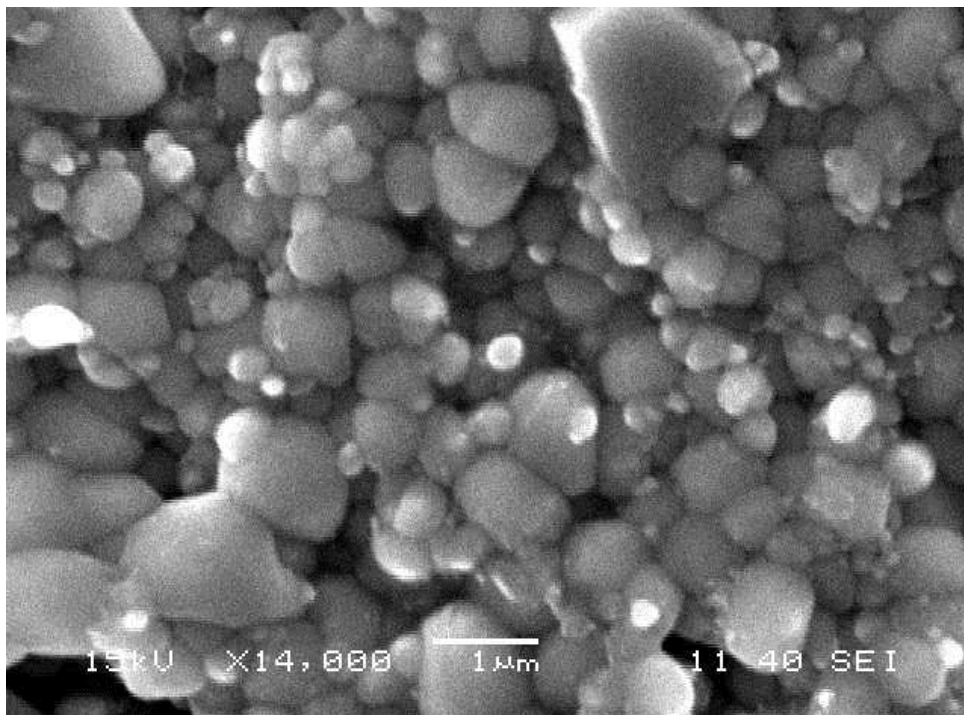


Fig. 3.3.1 SEM image of 48BZT-52BCT.

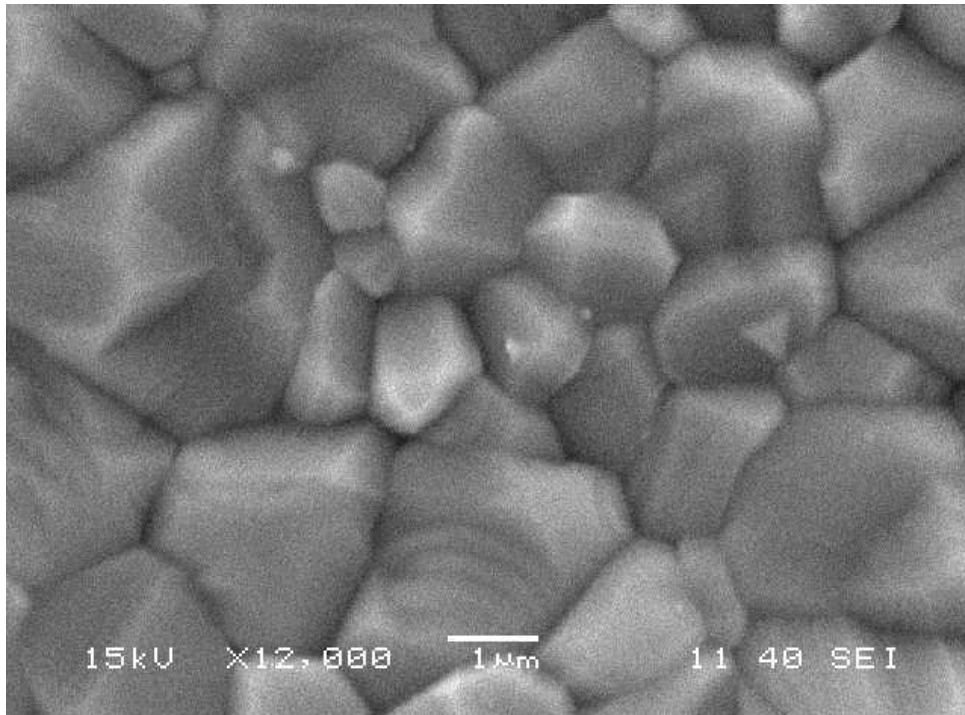


Fig 3.3.2 SEM Image of 50BZT-50BCT

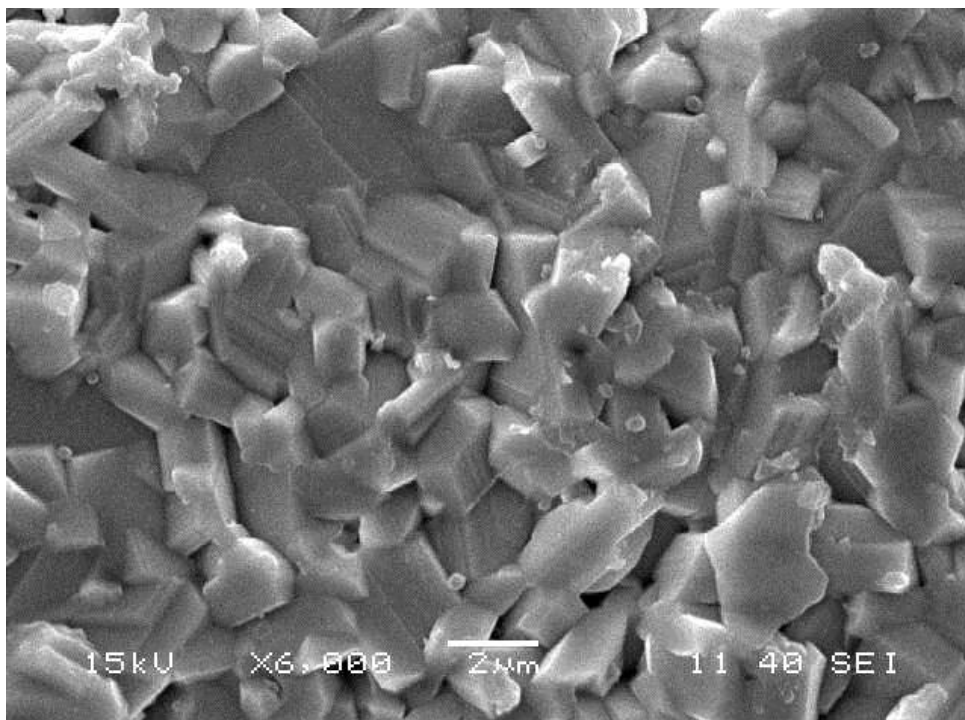


Fig. 3.3.3 SEM Image of 52BZT-48BCT.

From images 3.3.1, 3.3.2, 3.3.3 we can calculate the particle size. Fig. 3.3.1, depicts that particle size is $0.86\mu\text{m}$. The image shows few pores. From fig. 3.3.2, the particle size of

50BZT-50BCT is 1.7 μm . The sample is densely packed. Particle size of 52BZT-48BCT is 1.18 μm .

3.4 Dielectric Properties Analysis:

The change in dielectric constant with temperature is plotted below.

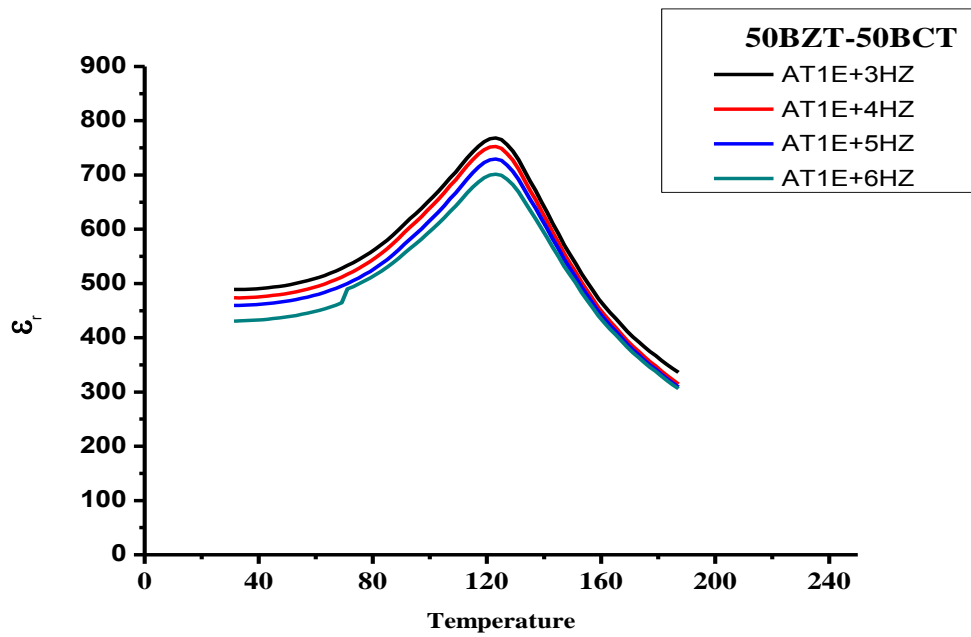


Fig.3.4.1 Graph between Dielectric Constant (ϵ_r) and Frequency of 50BZT-50BCT.

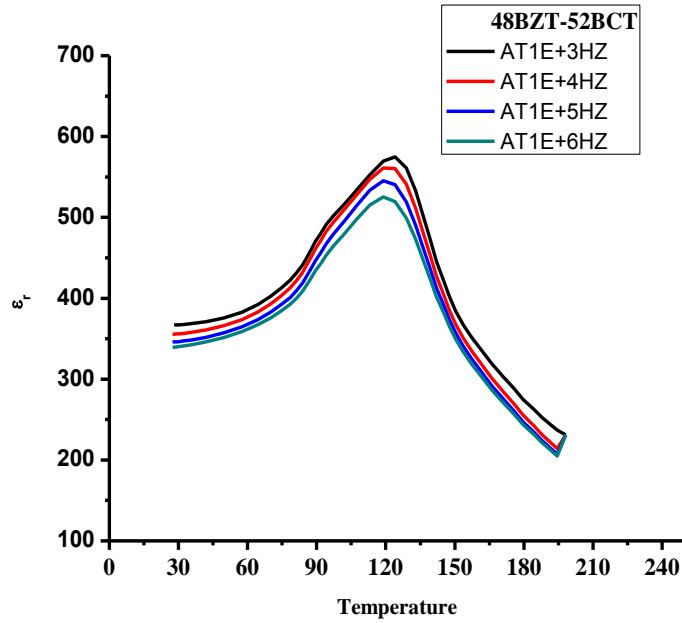


Fig.3.4.2 Graph between Dielectric Constant(ϵ_r) and Frequency of 48BZT-52BCT

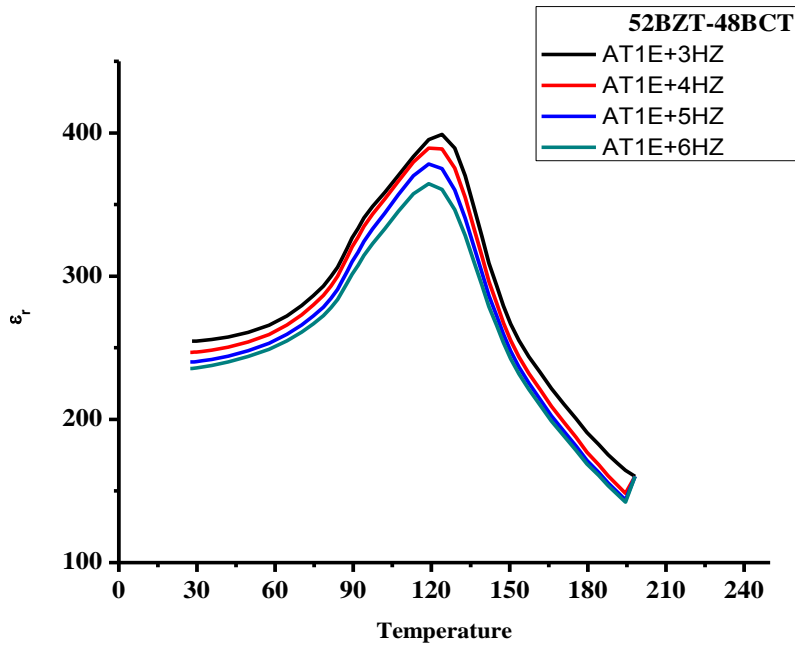


Fig. 3.4.3 Graph between Dielectric Constant(ϵ_r) and Frequency of 48BZT-52BCT.

From the above three graphs, we can conclude that the T_c is not sharp, it ranges around 118°C - 124°C, and dielectric constant (ϵ_r) is maximum in this region. The maximum dielectric constant at T_c is found to be 574.87, 768.39, 398.95 of 48BZT-52BCT, 50BZT-50BCT, 52BZT-48BCT respectively.

Initially with increase in temperature all the polarisations increases, as temperature supplies energy for the displacement of ions, atoms and electrons. Thus formation of dipoles is made possible. But slowly as the temperature is further increased, this energy causes randomness i.e., thermal agitation increases. And hence the polarisation and ϵ_r decreases.

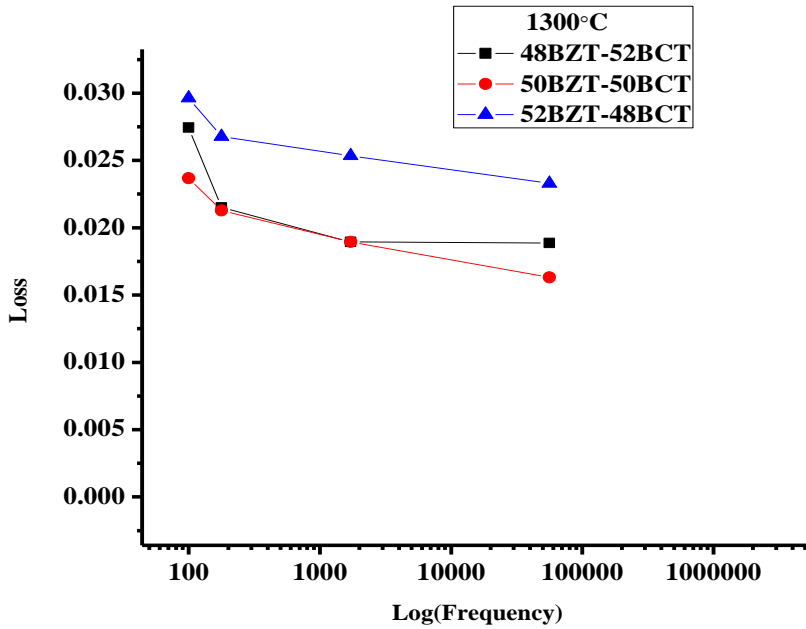


Fig. 3.4.4 Graph between Dielectric loss and Frequency of 48BZT-52BCT, 50BZT-50BCT,52BZT-48BCT sintered at 1300°C.

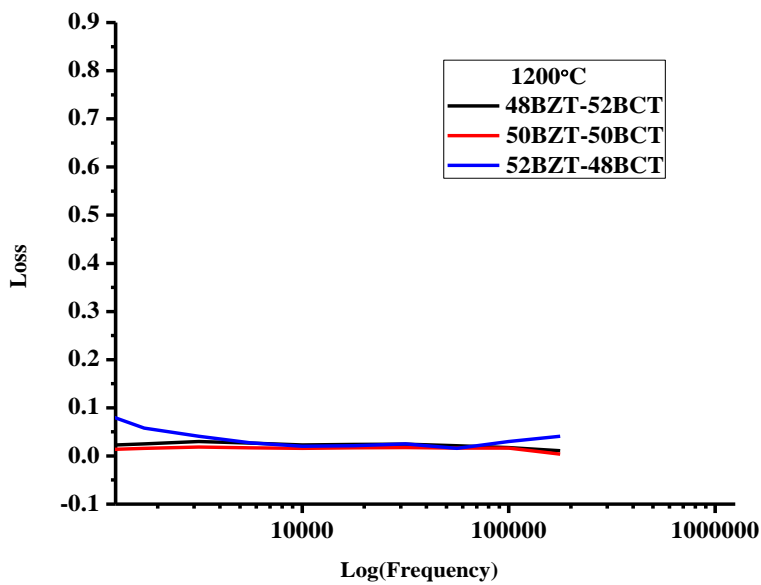


Fig. 3.4.5 Graph between Dielectric loss and Frequency of 48BZT-52BCT,50BZT-50BCT,52BZT-48BCT sintered at 1300°C

From graph 3.4.4 and 3.4.5, we find that dielectric loss decreases with increase in frequency. This can be explained from resonance frequency. Loss increases near resonance frequency. Here loss is decreasing with frequency, so we conclude that we are going away from the resonance frequency. The loss at 1 MHz frequency is 0.01 order for all the three compositions sintered at 1300°C and the 0.09 – 0.15 order for the compositions sintered at 1200°C.

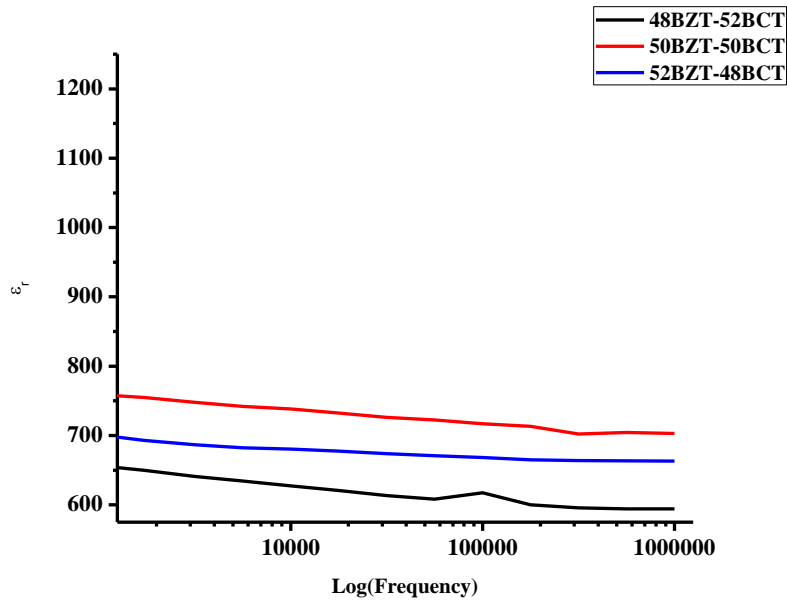


Fig. 3.4.6 Graph between ϵ_r and Frequency of 48BZT-52BCT,50BZT-50BCT,52BZT-48BCT sintered at 1200°C.

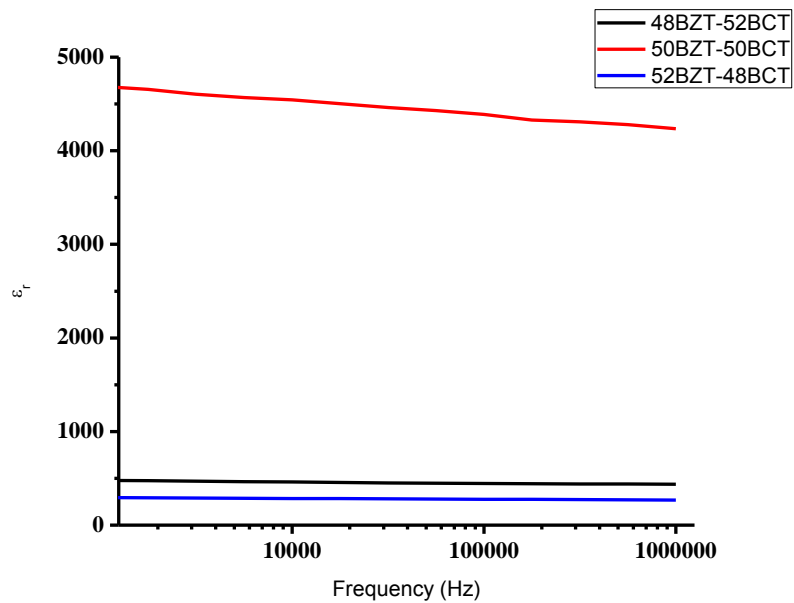


Fig. 3.4.7 Graph between ϵ_r and Frequency of 48BZT-52BCT,50BZT-50BCT,52BZT-48BCT sintered at 1300°C.

From plots 3.4.6 and 3.4.7, we conclude that at lower frequency all kinds of polarisation take place. But as we increase the frequency, slowly the polarisation's filters out. Only electronic polarisation remains because electrons are lighter than atoms and molecules so they can cope with the increase in frequency. This is further supported by the fig. 3.4.6 below.

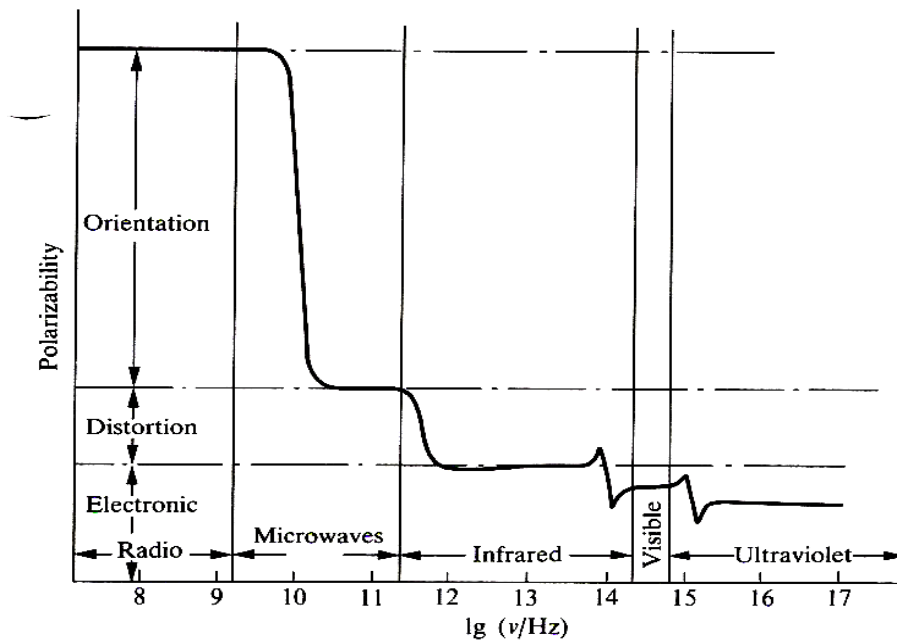


Fig. 3.4.8 Graph between Polarizability and Frequency.

3.5 Hysteresis Loop Analysis:

Hysteresis loops of the samples are depicted below.

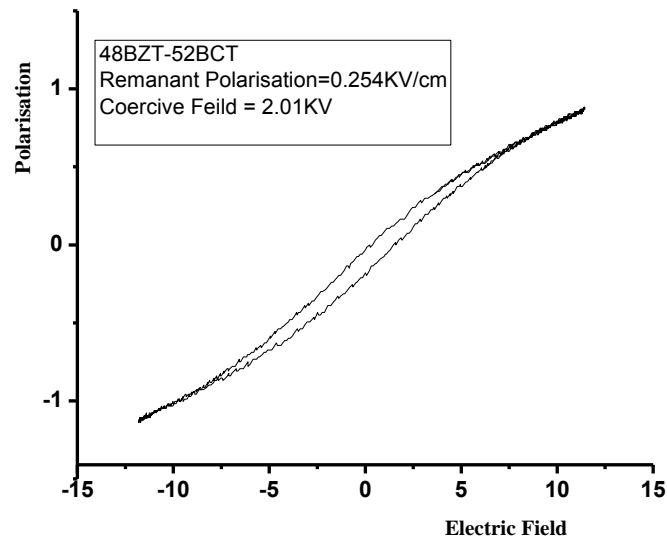


Fig. 3.5.1 PE Loop of 48BZT-52BCT at 1200°C.

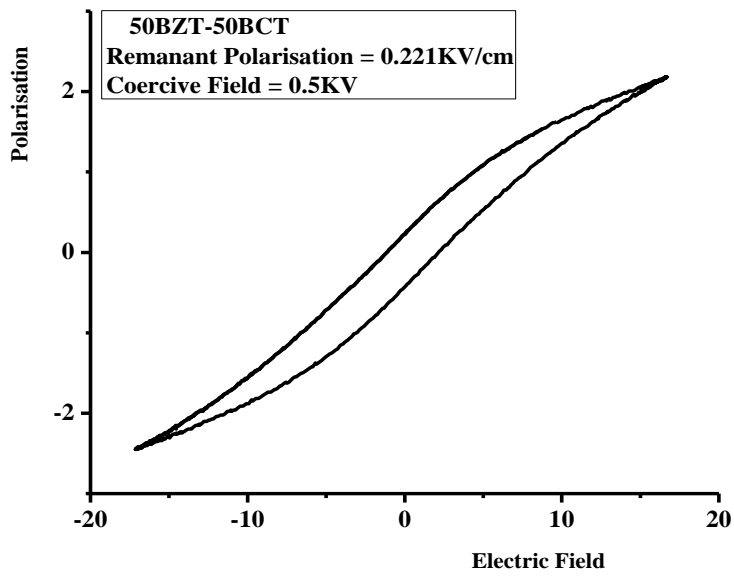


Fig. 3.5.2 PE Loop of 50BZT-50BCT at 1200°C.

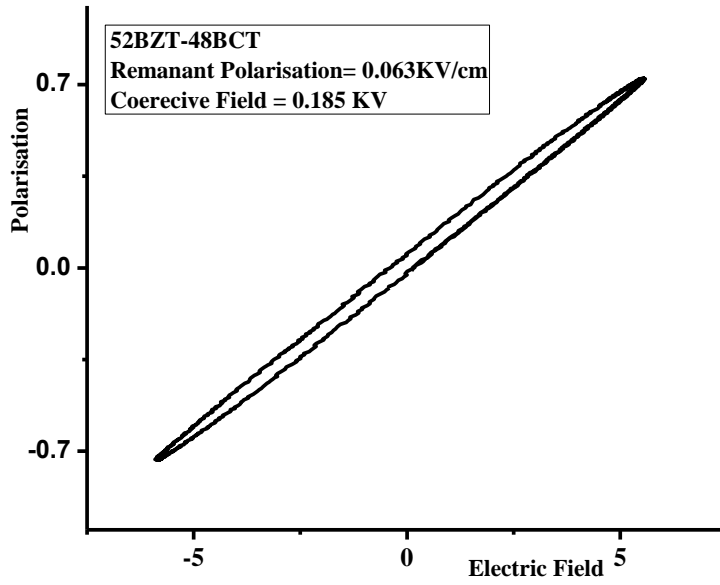


Fig. 3.5.3 PE Loop of 52BZT-48BCT at 1200°C.

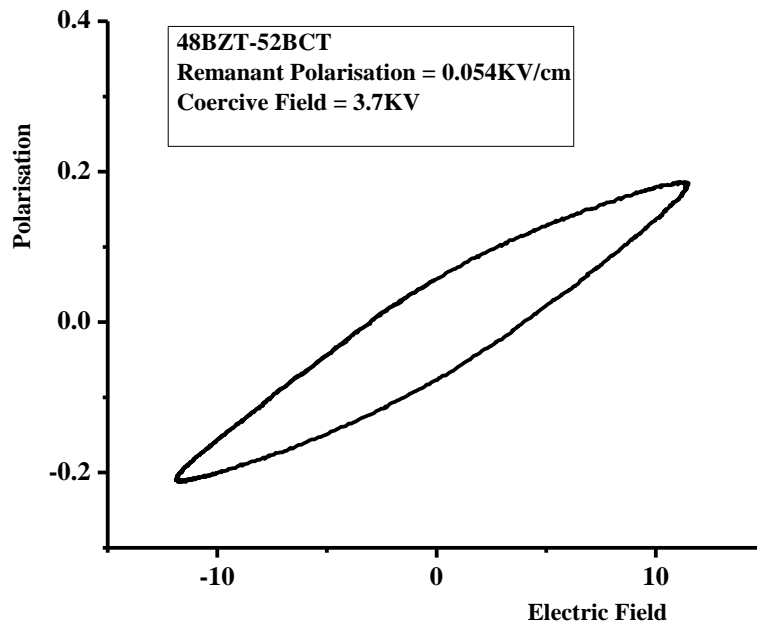


Fig.3.5.4 PE Loop of 48BZT-52BCT at 1300°C.

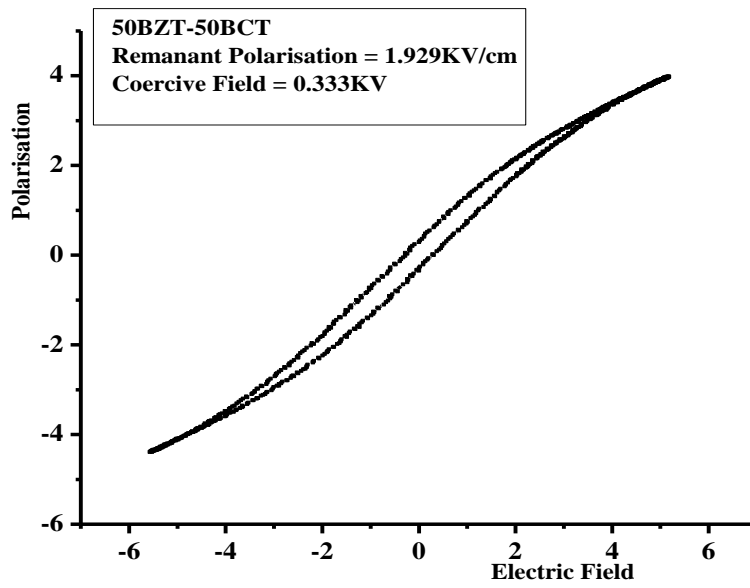


Fig. 3.5.5 PE Loop of 50BZT-50BCT at 1300°C.

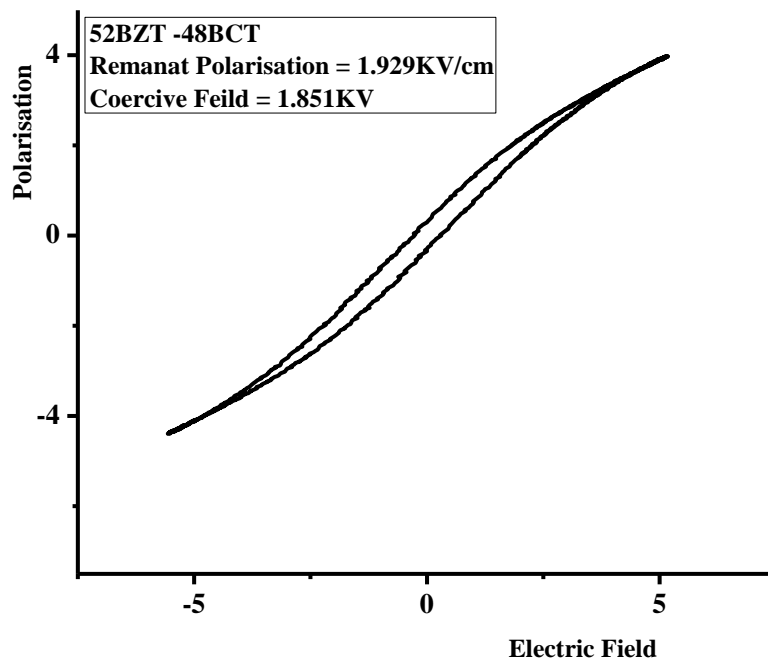


Fig 3.5.6 PE Loop of 52BZT-48BCT at 1300°C.

All the six figures above are the PE Loops of 48BZT-52BCT, 50BZT-52BCT, 52BZT-48BCT sintered at 1200°C and 1300°C. The existence of PE loop depicts that the material is ferroelectric. But the PE Loop of the material is slimmer. This feature is because of the presence of MPB region. From the figures we infer that the remnant polarisation ranges from 0.054 KV/cm – 1.929 KV/cm and coercive field value varies from 0.185 KV/cm – 3.7 KV.

Chapter 4: Conclusions

The three compositions (48BZT-52BCT, 50BZT-50BCT, 52BZT-48BCT) near MPB region was successfully prepared by sol-gel route. The XRD patterns of the compositions, confirmed single perovskite phase formation. The three compositions belonged to cubic crystal system. The density measurement revealed that, the best sintering temperature was 1300°C, as the density of all three compositions were better than those of 1200°C. The SEM images showed the grain size ranging from 800 nm to 1.8µm. The dielectric constant (ϵ_r) versus temperature showed diffused phase transition nature of 48BZT-52BCT, 50BZT-50BCT and 52BZT-48BCT. The dielectric loss and dielectric constant decreased with increase in frequency. The dielectric loss was found to be minimum at high frequency. The slim nature of hysteresis loop hinted about the relaxor nature of 48BZT-52BCT, 50BZT-50BCT and 52BZT-48BCT ceramics.

In sol gel route, we have reduced the sintering and calcining temperatures. The calcining temperature in solid state reaction method for the same (1-x)BZT-xBCT system is 1300°C but in chemical route it was 1100°C . Similarly the best sintering temperature in the dry media reaction method is 1400°C whereas in our procedure it was 1300°C.

From the above analysis, we conclude that best composition is 50BZT-50BCT sintered at 1300°C. The density of this composition is 4.65, highest amongst all and minimum porosity of 20%. The ϵ_r of 50BZT-50BCT is 770. The PE loop of this sample confirms it ferroelectric nature.

REFERENCES

1. S.O.Pillai, Solid State Physics, 6th ed. (New Age International Publishers Ltd.,2009).
2. Safari *et al.*, Ferroelectric Ceramics: Processing, Properties and Applications (Department of Ceramic Science and Engineering, Rutgers University, USA).
3. W. J. Merz, Physical Review Letter, **91**, 513 (1953).
4. Y. Xu, Ferroelectric Materials and their Applications (North Holland, Amsterdam, 1991).
5. R. E. Nettleton, Ferroelectrics, **1**, 3, 87, 93, 111, 121,127, 207, 221 (1970).
6. R. E. Nettleton, Ferroelectrics, **2**, 5, 77, 93 (1971).
7. Y. Saito *et al.*, Nature (London), **432**, 84 (2004).
8. T. R. Shrout and S. J. Zhang, J. Electroceram. ,**19**, 113(2007).
9. T. Takenaka and H. Nagata, J. Eur. Ceram. Soc., **25**, 2693 (2005).
10. Liu W., Ren X., Physical Review Letters, **103**, 257602 1-4 (2009).
11. H. X. Fu and R. E. Cohen, Nature (London) ,**403**, 281(2000).
12. M. Ahart et al., Nature (London) ,**451**, 545 (2008).
13. <http://www-phlam.univ-lille1.fr/pub/f/themas/phot/materiaux/Methode%20sol%20eng.htm>:
14. Dislich, H., Glastechn. Ber., **44**, 1(1971).
15. Kong LB *et al.*, Progress in synthesis of ferroelectric ceramic materials via high-energy mechanochemical technique, Prog Material Sceince(2007), doi: 10.1016/j.pmatsci.2007.05.001.
16. Bouledjnib L., Sahli S., M.J. CONDENSED MATTER , **12**, 199